Effect of rare-earth elements on nanophase evolution, crystallization behaviour and mechanical properties in Al–Ni–R (R = La/Mischmetal) amorphous alloys

K L SAHOO*, AMITAVA MITRA and SUKOMAL GHOSH

National Metallurgical Laboratory, Jamshedpur 831 007, India
*Corresponding author. E-mail: klsah@nmlindia.org

Abstract. The crystallization behaviour and evolution of nanoparticles in amorphous Al–Ni–Mischmetal (Mm) and Al–Ni–La alloys during heat treatment have been studied. Rapidly solidified ribbons were obtained by induction melting and ejecting the melt onto a rotating Cu wheel in an Ar atmosphere.

The crystallization behaviour of the melt-spun ribbons was investigated using differential scanning calorimetry and X-ray diffractometry (XRD). XRD studies confirmed that all the ribbons were fully amorphous. Al–Ni–Mm systems showed a three-stage crystallization process whereas Al–Ni–La system, in general, showed a two-stage crystallization process on annealing. Crystallization kinetics was analysed by Kissinger and Johnson–Mehl–Avrami approaches. In Al–Ni–La alloys, the crystallization pathways depend on the La concentration. Microhardness of all the ribbons was examined at different temperatures and correlated with the corresponding evolution of phases.

Keywords. Aluminium-based amorphous alloys; melt spinning; crystallization behaviour; microhardness.

PACS Nos   61.43; 81.30.D; 81.40.N; 81.40.

1. Introduction

Al-based amorphous alloys, in particular, based on Al-transition metal – rare earth systems are promising candidates as structural materials for industrial applications because of their high specific strength combined with good bending ductility [1,2]. In addition, these alloys also exhibit greater hardness [3] and wear [4] resistance. The mechanical properties can be further improved by ensuring uniform distribution of fcc-Al nanoparticles in the amorphous matrix by appropriate heat treatment [5]. The favourable mechanical properties of the alloy deteriorate if the size of the precipitates exceeds the range by a few nanometers. Growth of crystallites can be retarded by the choice of the alloy composition that leads to higher activation energy of crystallization. In several Al-based amorphous alloys, the formation of nanoscale Al particles and their crystallization kinetics have been studied by many

research groups [5–8]. Gangopadhyay and Kelton [9] investigated the crystallization process in Al–Ni–RE (RE = La/Mm) amorphous alloys and found that crystallization products depend upon the radius of the rare earth atoms. In the present paper, nanophase evolution, crystallization pathways and development of microhardness upon annealing of $Al_{88}Ni_7Mm_5$ (Mm = Mischmetal) and Al–Ni–La, containing 8 at% Ni and varying amount of La have been investigated.

2. Experimental

Ingots of composition $Al_{88}Ni_7Mm_5$ (denoted by Mm5), $Al_{88}Ni_8La_4$ (La4), and $Al_{87}Ni_8La_5$ (La5) were prepared by alloying the pure elements (purity of Al: 5N; Ni: 4N; La: 3N) by induction melting under a purified argon atmosphere. Mischmetal contains 55 mass% Ce, 25 mass% La, 10 mass% Nd, 7 mass% Pr and 3 mass% Fe. The microstructure of the ingot was examined by scanning electron microscopy (SEM) and phases were identified by X-ray diffractometry (XRD). Each ingot was inductively re-melted and melt-spun ribbons were prepared by ejecting the melt onto a rotating copper wheel in an Ar atmosphere.

The crystallization behaviour of the ribbons was studied by differential scanning calorimetry (DSC). The isochronal DSC study was conducted at different heating rates ranging from 10 to 40 K/min. For scanning at a constant heating rate, a second scan on the same sample was used as a baseline. For isothermal DSC analysis, the amorphous ribbons were heated at a rate of 100 K/min to the desired temperature up to 20 min before rapidly cooling to room temperature. After the isothermal DSC experiment, the same samples were investigated by XRD. From the XRD patterns the structure of the crystalline phases was determined. The evolution of hardness with temperature was investigated using a microhardness tester applying a load of 0.2 N.

3. Results and discussion

All the ingots used for melt-spinning were investigated by XRD (not shown) and SEM (representative microstructure is shown in figure 1). The phases present in the Al–Ni–La ingot are mainly identified as α-Al, $Al_{11}La_3$, Al_3La and Al_3Ni. SEM studies revealed that the primary $Al_{11}La_3$ and Al_3Ni phases are uniformly distributed in the matrix of α-Al and a small volume of ternary-Al–$Al_{11}La_3$–Al_3Ni eutectic (figure 1). In Mm5 ingot, the phases present are α-Al, $Al_{11}RE_3$, Al_3RE, Al_3Ni and small amounts of other phases.

All the melt-spun ribbons show good bending ductility. XRD studies revealed that all the ribbons were fully amorphous on the substrate side (not shown) as well as on the air-cooled side (figure 2). All the as-melt-spun ribbons showed a distinct broad and a small diffuse maximum centred around 37° and 66°, respectively, which are characteristics of a glassy phase.

The ribbons are heated continuously in a DSC at various heating rates. Figure 3 shows the representative DSC curves of the amorphous alloys heated at a rate of 40 K/min. The number of heat events as well as their position on the
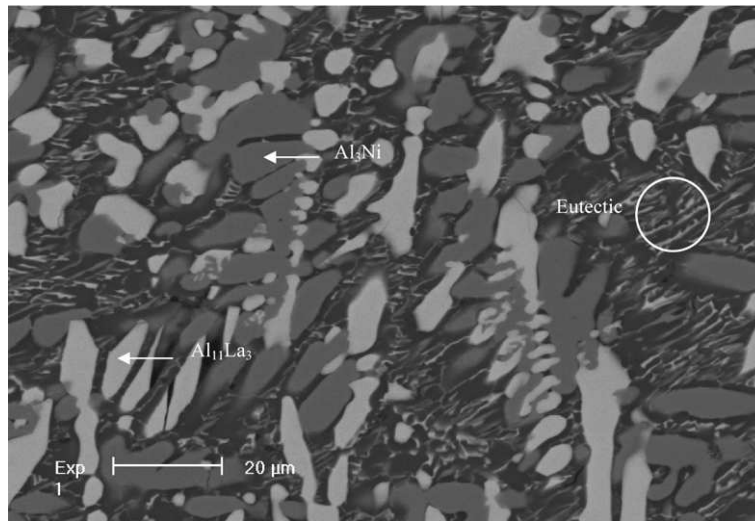
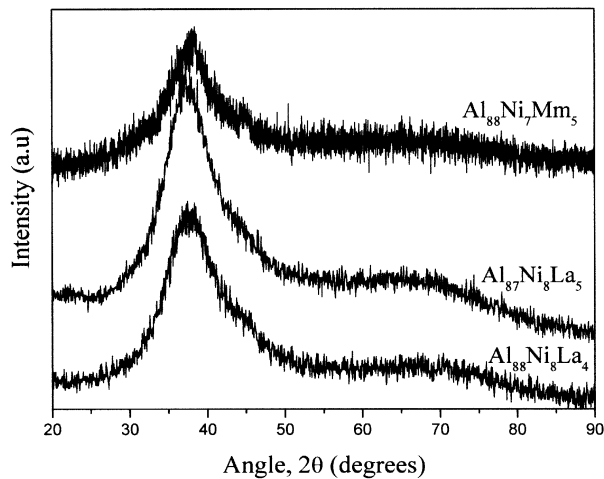**Figure 1.** SEM back-scattered image of $Al_{87}Ni_8La_5$ ingot, the phases are marked.

Figure 2. XRD patterns of as-melt-spun Al–Ni–RE amorphous ribbons on the air-cooled side.

temperature axis change with alloy composition. Two or three exothermic peaks corresponding to the crystallization of phases are observed in different temperature ranges. Mm5 amorphous alloy undergoes three stages of crystallization processes whereas Al–Ni–La amorphous alloys undergo two stages of crystallization processes. The crystallization peak temperature (T_p) at different heating rate is shown in table 1. In Al–Ni–La amorphous alloys, the first T_p increases whereas the second T_p decreases with increasing La content. The peak temperatures of crystallization increases with increasing heating rate (table 1) which leads to the determination of
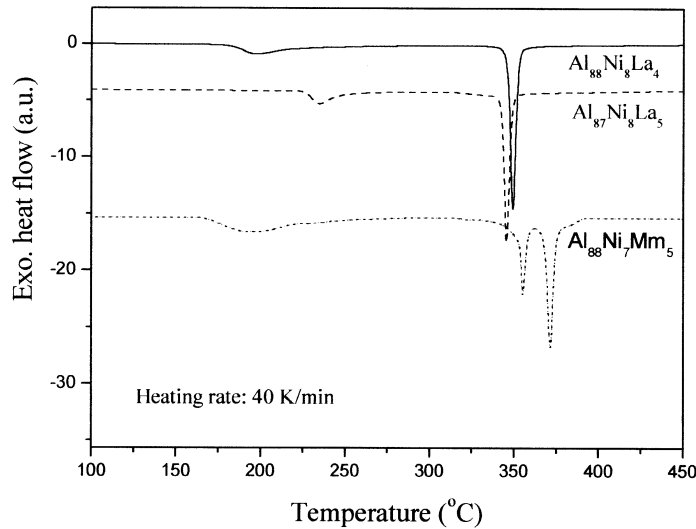
Figure 3. DSC curves of amorphous Al–Ni–RE (RE = La/Mm) alloys at a heating rate of 40 K/min.

activation energies (E_a) of the crystallization stages by Kissinger analysis [10]:

$$\ln\left(\frac{T_p^2}{\beta}\right) = \left(\frac{E_a}{RT_p}\right) + A,$$

where β is the heating rate, T_p is the peak temperature in Kelvin, R is the gas constant and A is a constant. The values of activation energies for all crystallization stages are shown in table 1.

In order to identify the appearance of different phases responsible for the crystallization stages in the DSC curve, different samples were heated in the DSC up to the end of the individual heat events and the same samples were analysed by XRD. The first crystallization stage in La4 and La5 alloys is due to the formation of fcc-Al. The second crystallization stage in these alloys is due to the formation of $Al_{11}La_3$, Al_3La and Al_3Ni. In Mm5 alloy, the first crystallization stage is due to the formation of fcc-Al from the amorphous matrix, the second crystallization stage is due to the formation of $Al_{11}RE_3$ and the third crystallization stage is due to the formation of Al_3Ni and other intermetallic compounds containing rare earth elements.

The crystallization behaviour of the phases that formed during different stages of crystallization was investigated through isothermal DSC studies. Different samples were annealed at different temperatures around the onset of temperature of the crystallization stages (isothermal curves are not shown). The isothermal phase transformation is generally described by the well-known Johnson–Mehl–Avrami (JMA) transformation kinetic equation [11,12]:

$$x = 1 - \exp[-\{K(t - t_0)\}^n],$$

Table 1. Peak temperatures at different heating rates and activation energy of the alloys.

Alloy system	Crystalliza-tion stages	Peak temperature (°C) at different heating rates				E_a (kJ/mol)
		10 K/min	20 K/min	30 K/min	40 K/min	
La4	1st peak	186	192	195	197	207±12
	2nd peak	329	339	345	349	200±1
La5	1st peak	224	229	232	235	258±7
	2nd peak	325	335	341	345	201±1
Mm5	1st peak	182	184	192	193	129±6
	2nd peak	339	348	349	355	288±6
	3rd peak	350	362	364	371	256±4

where x denotes the transformed volume fraction at time t, n is the JMA exponent, which depends on nucleation rate and growth kinetics, K is the reaction rate constant and t_0 is the time lag. The n values were calculated for the range of data between $x = 0.01$ and $x = 0.5$. For Mm5 alloy, the average Avrami exponent for the first stage of crystallization is 1.4 which according to Christian's [13] classification indicates that the precipitates grow from nuclei which are already present in the as-melt-spun ribbons. The n value for the second stage of crystallization of Mm5 alloy is 3.9. Similarly, for La5 alloy the average value of n for the first and second crystallization stages are 2.5 and 3.6, respectively. Different values of Avrami exponent are index of different types of nucleation and growth mechanism, e.g., $n = 1.5$ is indicative of three-dimensional growth with zero nucleation rate, $n = 1.5$–2.5 refer to growth with decreasing nucleation rate, $n = 2.5$ advocates for constant nucleation rate and $n > 2.5$ postulates three-dimensional growth with increasing nucleation rate [13].

Figure 4 shows the variation of microhardness with temperature. Individual ribbons were annealed for 10 min at temperatures ranging from room temperature to 480°C. The heating rate up to the annealing temperature was 100 K/min. The hardness values shown in figure 4 are the average of about 10 measurements on each sample and the corresponding errors are shown for each data point. The as-melt-spun ribbons show higher hardness with increasing RE elements concentration (figure 4) indicating different initial microstructures of the ribbons. During annealing, hardness does not change much from room temperature to about 150°C. This is due to the fact that the microstructures do not change appreciably as these glasses are thermally stable at lower temperatures. Thereafter, a sharp increase of hardness with increasing temperature is observed which is caused by crystallization of fcc-Al leading to precipitation strengthening of the material. The highest hardness values were detected at around 290°C for La4 and La5 alloys and at around 300°C for alloy Mm5. At the point where the highest hardness is observed the matrix is still amorphous with supersaturated solute elements. Crystallization at higher temperatures (above 290°C for La5 alloy) results in a sharp drop of hardness owing to substantial growth of Al particles and decomposition of the amorphous
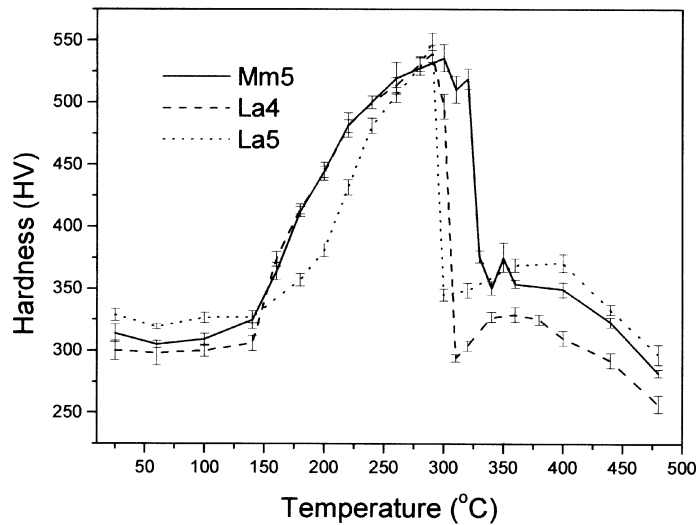
Figure 4. Isochronal microhardness evolution of different Al–Ni–RE ribbons. The samples were annealed for 10 min at each measuring temperature.

matrix leading to precipitation of intermetallic particles (mainly, $Al_{11}La_3$ and Al_3Ni) from the matrix. With the progress of crystallization, hardness increases again due to increased volume fraction of crystallized intermetallic particles. Later on, the observed decrease in hardness with higher temperature is contemplated due to coarsening of the particles.

4. Conclusions

$Al_{88}Ni_7Mm_5$ alloy undergoes three-stage crystallization process whereas $Al_{88}Ni_8La_4$ (La4) and $Al_{87}Ni_8La_5$ (La5) alloy undergo two-stage crystallization process. The two stages of crystallization in La4 and La5 alloy correspond to the formation of fcc-Al and $Al_{11}La_3$, Al_3Ni, Al_3La, respectively. The three stages of crystallization in Mm5 alloy corresponds to the formation of fcc-Al, $Al_{11}RE_3$, and Al_3Ni plus other intermetallic compounds, respectively. The results showed that the variation of La content has significant influence on the crystallization pathways from amorphous to stable crystalline phases and on the evolution of nanophases with temperature. The first crystallization temperature increases while the second one decreases with increasing La concentration.

The hardness does not change appreciably up to a temperature of 150°C indicating the structural stability at lower temperatures. Thereafter, the sharp increase in hardness is due to nanoscale precipitation of fcc-Al. The rapid fall of hardness in La4 and La5 alloys after 290°C and in Mm5 alloy after 300°C is due to the decomposition of amorphous matrix and the formation of intermetallic compounds.

Acknowledgement

References

[1] A Inoue, T Zhang, K Kita and T Masumoto, *Mater. Trans. JIM.* **30**, 870 (1989)
[2] Y He, S J Poon and G Shiflet, *Science* **241**, 1640 (1988)
[3] Z C Zhong, X Y Jiang and A L Greer, *Philos. Mag.* **B76**, 505 (1997)
[4] T Gloriant and A L Greer, *Nanostruc. Mater.* **10**, 389 (1988)
[5] A Inoue, *Prog. Mater. Sci.* **43**, 365 (1998)
[6] F Ye and K Lu, *J. Non-Cryst. Solids* **262**, 228 (2000)
[7] D R Allen, J C Foley and J H Perepezko, *Acta Met.* **46**, 431 (1998)
[8] K L Sahoo, V Rao and A Mitra, *Mater. Trans.* **44**, 1075 (2003)
[9] A K Gangopadhyay and K F Kelton, *Philos. Mag.* **A80**, 1193 (2000)
[10] H E Kissinger, *Anal. Chem.* **29**, 1702 (1957)
[11] W A Johnson and R F Mehl, *Trans. Am. Inst. Min. Metall. Engg.* **135**, 416 (1939)
[12] M Avrami, *J. Chem. Phys.* **9**, 177 (1941)
[13] J Christian, The theory of transformation in metals and alloys – Part 1, *Equilibrium and general kinetic theory* (Pergamon Press, Oxford, 1975) p. 542